

CRYO-ELECTRON MICROSCOPY OF VITRIFIED WATER

J. Dubochet and J. Lepault

*European Molecular Biology Laboratory (EMBL), Meyerhofstrasse 1,
6900 Heidelberg, F.R.G.*Résumé

L'eau liquide peut être aisément vitrifiée en une forme favorable à la cryo-microscopie électronique. La glace cubique peut aussi être obtenue par refroidissement rapide du liquide. L'eau vitreuse obtenue à partir du liquide et l'eau amorphe solide (H_2O_{as}) obtenue par condensation de la vapeur, semblent être identiques sur la base de leurs diffractogrammes, de leur température de cristallisation et de leur densité. La glace, au-dessus d'environ 70 K, est très résistante à l'irradiation électronique mais, en dessous de cette température, est transformée par une dose de seulement quelques centaines d'électrons par nm^2 , en une substance amorphe ressemblant à l'eau vitrifiée.

Abstract

Liquid water can easily be vitrified in a form suitable for cryo-electron microscopical observations. Cubic ice can be formed by rapid cooling of the liquid. As judged by a comparison of the electron diffractograms, by the determination of the crystallization temperature and by density measurements, vitrified water obtained by cooling the liquid appears identical to solid amorphous water (H_2O_{as}) obtained by vapour condensation. Ice is resistant to the electron beam above ca. 70 K but below this temperature, for an irradiation of some hundreds of electrons per nm^2 , it is transformed into an amorphous substance, similar to vitrified water.

Introduction

The idea of solidifying water or aqueous substances without changing their structure has stimulated science fiction writers, philosophers and scientists. Until recently it was the latter who got the smallest return for their efforts: liquid water always crystallized when cooled into a solid. This unsuccessful led to the idea that vitrification of liquid water is fundamentally impossible and that there is no continuous relationship between the liquid state and solid amorphous water obtained by vapour condensation [Review in (1)]. In 1980 Brüggeler and Mayer (2) changed the situation in succeeding the vitrification of small water droplets by spraying them at high pressure in a cryogen. Shortly after and independently we found another method especially suitable for electron microscopical work (3). The old hypothesis that water vitrifies when the cooling rate is high enough was thus confirmed. It is the good fortune of the electron microscopist that, reducing sample size in order to increase the cooling speed, vitrification becomes easy just when the dimensions of the specimen are those suitable for electron microscopy. This situation opens a new and beautiful field for electron microscopy (4,5). It has also allowed us to gather some new observations on solid water. Most of them have been published but, in journals which are not always accessible to the specialists (6,7,8,9). In the present article we have put together all our observations on pure water, and complemented some of them.

Vitrification of Liquid Water

Among several variants that we use routinely, the following method is the simplest to describe. A copper grid (hole dimension: $100\text{ }\mu\text{m}$) is held by tweezers fixed on a guillotine about 10 cm above a small recipient containing two cm^3 of liquid ethane cooled in a bath of liquid nitrogen. The cleaned copper grid is uncoated. A drop of pure water or of any aqueous solution is put on the grid, most of it is removed by pressing a blotting paper towards the grid for about 1 sec and the guillotine is released allowing the grid to fall down into the cryogen. The grid is then transferred to liquid nitrogen (where it can be stored) and from there into the cryo-specimen holder where it is kept cold during transfer and subsequent observation in the electron microscope. With this method many squares of the grid are filled with a thin vitrified water layer of usable thickness (less than 200 nm). Other variants of the method consist in using a grid coated with a perforated carbon film. The thin water layer is then formed across the ca. $2\text{ }\mu\text{m}$ diameter holes of the carbon film. A thin and uniform water layer can also be obtained on a continuous carbon film, pretreated by a glow discharge in alkylamine vapour (10). Finally, small water droplets can be sprayed on a hydrophilic carbon film and immersed into the cryogen within the next 100th of a second (6). All these methods can be used routinely with a success rate comparable to the most traditional electron microscopy specimen preparation procedures.

General Properties

Three forms of solid water are seen by electron microscopy. They are depicted, together with their electron diffractogram, in Fig.1.

a) Hexagonal ice crystals are always relatively large (μm), they are rich in visible structures like grain boundaries, bent contours and dislocation networks. By electron diffraction they present several reflections which are typical for this form of ice [(100) corresponding to a plan spacing of 0.389 nm and (101) corresponding to 0.343 nm]. b) Cubic ice crystals are always in the 100 nm range, leading to a grainy appearance in the direct image. They present thus a powder electron diffractogram. It should be noticed that all the reflections of cubic ice also exist in hexagonal ice and it is therefore the absence of some reflections of hexagonal ice, such as those mentioned above, which allows the unambiguous characterization of the cubic form. Noteworthy is also the shoulder on the inside of the first ring (111) suggesting a minor contribution of the (100) reflection of hexagonal ice. Judging by the width of the rings, we have never detected cubic ice crystals smaller than ca. 30 nm. c) As expected, vitreous ice is characterized in the direct image by its total absence of structure. Indeed, down to a resolution of 2 nm the photographic grain distribution in a micrograph of a thin layer of vitrified water is indistinguishable from the distribution obtained by irradiating the photographic film in absence of a specimen (of course vitrified water has a normal electron scattering cross-section). By electron diffraction, amorphous ice has, however, a very characteristic structure formed by a number of diffused rings with well-defined radius and width (see below).

When pure water is prepared as described above, the regions of the specimen with a thickness adequate for electron microscopy are generally vitrified. The thicker regions which are at the limit of visibility in the electron microscope at the voltage we are using (up to 120 kV), are frequently crystallized. From this, we infer that the method is capable of vitrifying water up to the micrometer range.

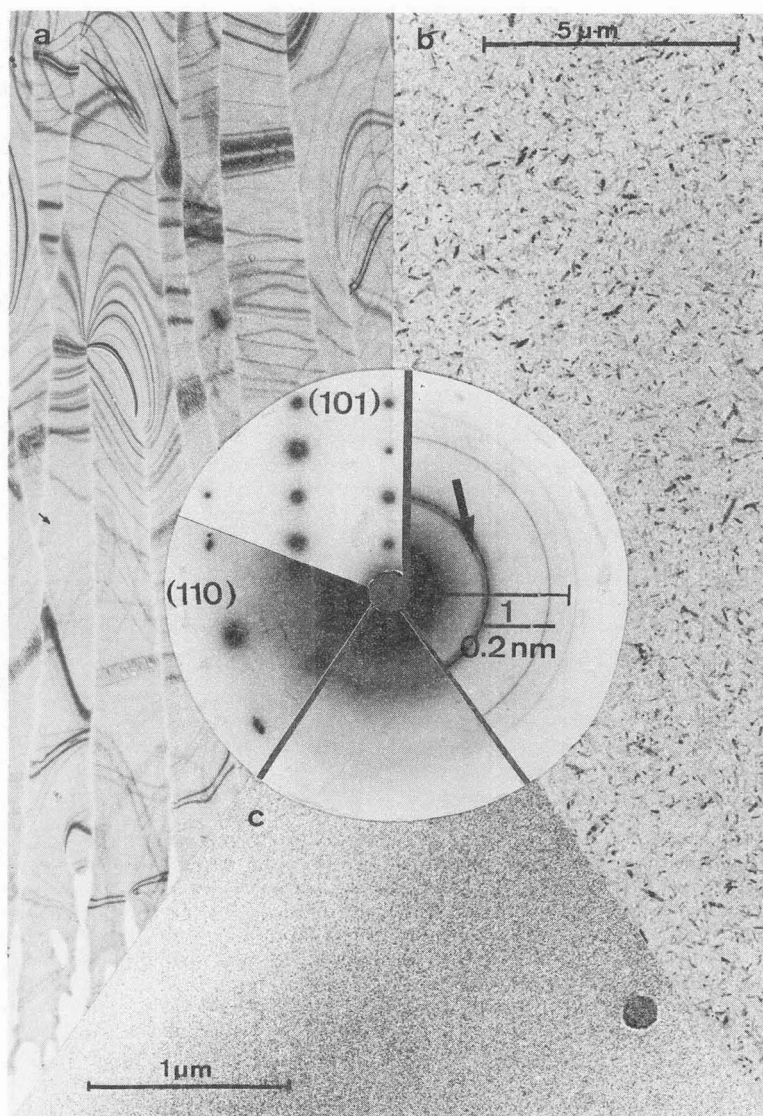


Figure 1 Typical images and electron diffractograms of the three forms of ice that can be observed in the electron microscope. The direct images are printed at a magnification of $\times 10,000$ (a,b) and $\times 100,000$ (c). (a) Hexagonal ice obtained by rapid freezing of a thin water layer spread on a carbon film. The thickness of the layer shown on the micrograph is 50-80 nm. The diffractograms which are taken from other specimens show the (110) and (101) planes. (b) Cubic ice obtained by warming a layer of solid amorphous water. The weak contribution of the (100) form of hexagonal ice, has been marked on the diffractogram (arrow). The layer is approximately 70 nm thick. (c) Vitrified thin layer of pure water. The thickness is approximately 70 nm.
(From (6) with modifications.)

When the specimen is prepared under suboptimal freezing conditions, in particular when the cryogen is not at a low enough temperature, vitrification is not or only partially achieved. Fig.2 is an example of this frequently observed situation in which hexagonal, cubic and vitreous ice coexist. Of special interest is the presence of cubic ice under these conditions. It demonstrates that this form of ice, previously thought to be obtained only by crystallization of solid amorphous water (H_2O_{as}), can also be obtained by rapid cooling. In general, cubic ice_{as} occupies a small portion of the surface of the specimen, between zones of hexagonal and of vitreous ice. This observation could support the hypothesis that cubic ice formation is a preliminary step in the formation of hexagonal ice. The islands of hexagonal ice lost in a sea of vitreous ice probably indicate some heterogeneous nucleation phenomenon. They resemble, though on a smaller scale, the spherulites that Luyet liked so much (11).

Vitreous ice crystallizes into cubic ice upon rewarming. We have found (6) that the crystallization temperature T_c is around 135 K and is dependent on the warming rate, in agreement with X-ray measurements made on amorphous solid water (H_2O_{as}) by Dowell and Rinfret (12). We should note, however, that the specimen in an electron microscope is a difficult place to make precise temperature measurements. Consequently we do not attribute too much value to our measurements in the debate on T_c (see 13). What we see unambiguously, however, is that crystallization has the clear-cut properties of a phase transition. Watching the transition on the direct image shows the sudden appearance of cubic crystals which, once formed, remain unchanged upon further warming. The effect is even more obvious in the electron diffractogram where the diffuse rings of vitreous ice fade away while being replaced by the sharp rings of cubic ice, instead of the diffuse rings getting sharper and sharper until they are transformed into the cubic ice pattern. This fact is a strong indication that the formation of a cubic ice crystal is a sudden phenomenon after an internal energy threshold is attained and it involves a volume of at least 30 nm in diameter. Once the cubic ice crystals are formed, there is very little further change upon warming until evaporation becomes significant around 170 K. Measurements of the evaporation rate, though also suffering from the uncertainty of temperature measurements, are compatible with the known data on partial pressure of water at these low temperatures (6). In particular, we see no significant difference in the evaporation rate of cubic and of hexagonal ice.

Comparison of Vitrified Liquid Water and H_2O_{as}

A layer of H_2O_{as} is easily formed in the electron microscope. In fact, and without special precaution, residual water vapour, in the specimen chamber of the cryo-electron microscope, condenses on the cold specimen and forms an undesirable contaminating layer. In order to avoid this effect, we have built a special anticontamination trap, which limits this condensation to a negligible amount. This being established, it is easy to form thin layers of pure H_2O_{as} obtained by vapour condensation on a very thin carbon film (negligible compared to water) and to compare them with uncontaminated thin layers of vitrified liquid water. These two forms of water appear to be identical in all the aspects we have explored in the electron microscope (6,7,8). In particular:

1. The position and width of the first three rings in the electron diffractogram of the thin specimen are shown in Figure 3. This comparison is objective in the sense that it is made on the basis of

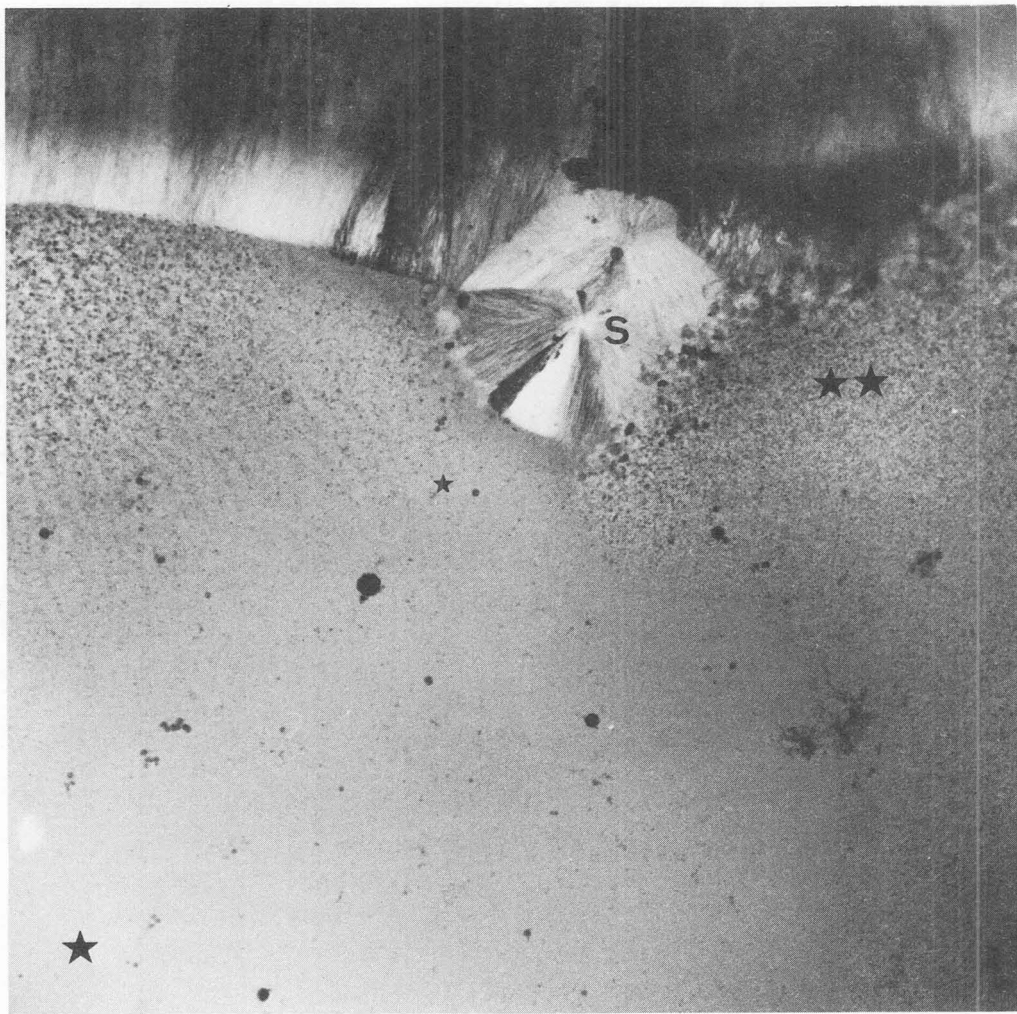


Figure 2 Thin layer of solid water at the edge of a grid hole. The water forms hexagonal, cubic crystals or is vitrified in the regions marked H,C and V respectively. A spherulite is marked S. The thickness is estimated to be around 100 nm in the region marked by one star and 300 nm in the region marked by two stars.

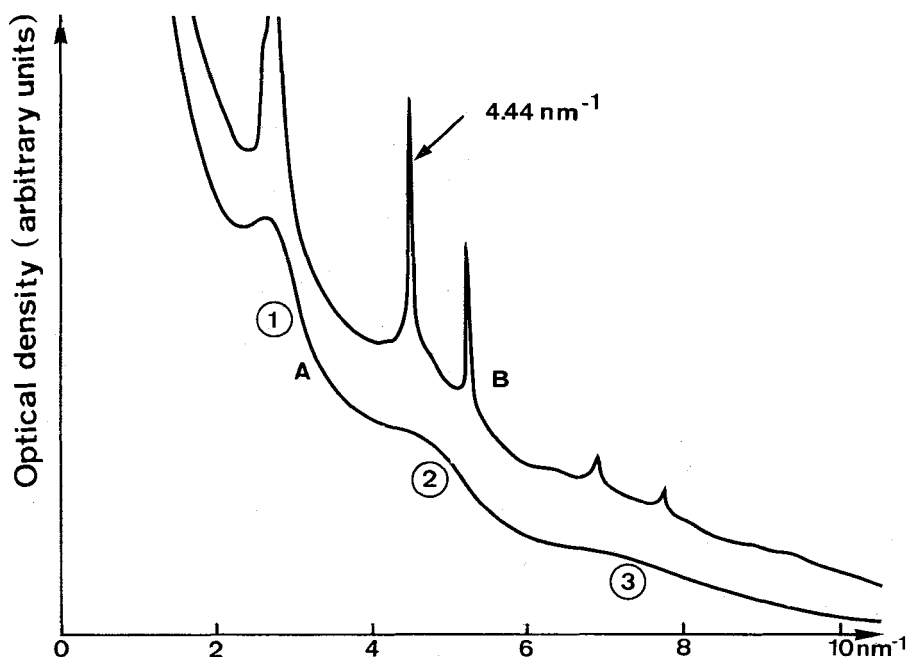


Figure 3 Characterization of the electron diffractogram of vitrified liquid water and solid amorphous water ($\text{H}_2\text{O}_{\text{as}}$) obtained by vapour condensation. The optical density of the electron diffractogram of vitrified water is shown in A where the first three rings are marked. After rewarming above the crystallization temperature, the layer exhibits the pattern of cubic ice shown in B. The ring (220) corresponding to a plane spacing of 0.225 nm is used for calibration. For clarity, the curves A and B have been translated vertically.

Vitrified Liquid				
	Position	FWHM	Position	FWHM
Ring 1	2.67 ± 0.10	0.63 ± 0.12	2.68 ± 0.06	0.56 ± 0.10
Ring 2	4.35 ± 0.13	0.96 ± 0.34	4.46 ± 0.13	0.91 ± 0.28
Ring 3	7.04 ± 0.30	1.41 ± 0.51	7.04 ± 0.30	1.30 ± 0.09

The table gives the average position and the full width at half maximum (FWHM) for the three rings indicated in curve A for vitrified liquid water and for similar diffractograms obtained from $\text{H}_2\text{O}_{\text{as}}$. In both cases, 5 electron diffractograms recorded at 80 kV with 670 mm camera length were digitized with an Optronics Photoscan P-1000 with 0.1 mm raster size. An iterative process fits the experimental curve obtained after one dimensional reduction of the two dimensional set of data, with a sum of 3 Gaussian curves and an inverse second order polynomial which represents the background. The starting value for the iterative procedure is taken from any reasonable approximation. It converges rapidly towards a single solution. The table gives the average center position and FWHM expressed in nm^{-1} ($1/d$), for the 3 fitted Gaussian curves. A fourth weak ring is distinguishable at a ca. 8.2 nm^{-1} .

(Redrawn from (8) with modifications.)

an objective test described in the Figure Legend. It is found that within the accuracy of the method, the diameter and the width of the ring are identical for the two types of specimen.

2. The crystallization temperature of $\text{H}_2\text{O}_{\text{as}}$ and of the vitrified liquid are the same to within the measurement error ($\pm 3^\circ$). Here again we are uncertain about the absolute value of T_c .

3. The density of vitrified liquid water can be determined from contrast measurements in the image of polystyrene spheres solution. The value we have measured is 0.93 ± 0.02 g per cm^3 . It agrees with the value of 0.94 ± 0.02 that Ghormley and Hochanandel found by flotation of $\text{H}_2\text{O}_{\text{as}}$ (14).

Electron Beam Damage

When observed in a liquid nitrogen cooled specimen holder, water seems to be a very stable substance. An electron dose which is very large compared to the dose required for one micrograph must be applied before significant changes take place. The beam-induced sublimation causes about 1 water molecule to be etched away each time the specimen is irradiated with a dose of 100 electrons at 100 kV (6,15). This effect is independent of the thickness of the specimen. It can be interpreted as a surface phenomenon in which the surface molecules are ejected each time they suffer an inelastic scattering event.

Beam-induced crystallization has been observed between 110 K and T_c . It causes irradiated areas to crystallize more rapidly than unirradiated areas. The colder the specimen, the higher the dose inducing crystallization. Below 110 K the crystallization dose becomes so high that the specimen is etched away before crystallization takes place.

Beam-induced evaporation and crystallization are not due to direct heating effects. This can be seen in that these effects are electron flux independent. They are also strictly limited to the irradiated area whereas heating effects would extend outside this area. The phenomenon of bubbling is also worth mentioning although it becomes important only when organic material is added to the water. It is not yet clear if water plays a direct role in the chemical reactions leading to the formation of the bubbles, or if it only prevents rapid diffusion of the radio-decomposition products of the organic material.

Electron beam damage below the temperature of liquid nitrogen is very different from above this temperature. The first difference is practical: cold stages working below liquid nitrogen temperature are rare and generally difficult to work with. We have made our observations in a conventional transmission electron microscope equipped with a liquid helium cryostat in which the specimen is kept at the temperature of 4.2 K and in a scanning transmission electron microscope (STEM) with a cryo-specimen holder which can be cooled down to 20 K by helium gas. As is the case for most STEM, this machine cannot provide high resolution (sharp) electron diffractograms, as the angular coherence of the beam is low.

The other difference is that water becomes very sensitive to the electron beam below 70K (9): ice crystals are destroyed by an electron dose which, depending on the temperature, is from 200 to 500 electron $\cdot \text{nm}^{-2}$. For comparison, this dose is not even sufficient to etch away one molecular layer at a higher temperature. This transformation leads to an amorphous material which has an electron

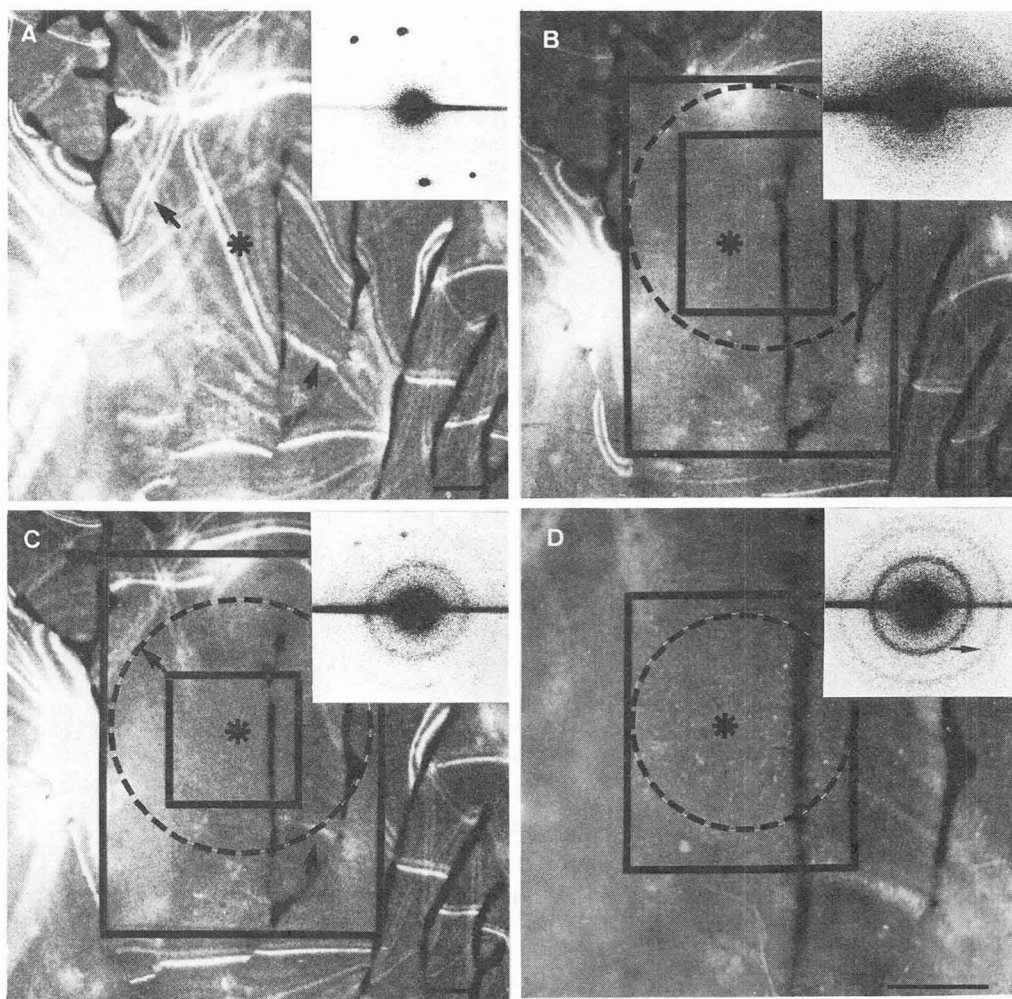


Figure 4 Thin layer of hexagonal ice irradiated below 70 K and warmed above recrystallization temperature in a STEM. (a) Direct image and corresponding electron diffractogram of the original specimen recorded at 40 K. (b) Same region after irradiation at 40 K. The area within the small rectangle has received $5000 \text{ e}^- \cdot \text{nm}^{-2}$ and the area within the large rectangle has received $1000 \text{ e}^- \cdot \text{nm}^{-2}$ in addition. The electron diffractogram of the dashed circle is shown in the insert. (c) Same sample after warming at about 155 K. Arrows mark the original bent contours which reappear in the intermediate region. The diffractogram of the dashed circle also shows the reappearance of the original hexagonal crystal and cubic ice. (d) Enlarged view of the centre of the field shown in (c). The central region has the grainy structure of cubic ice. The electron diffractogram of the dashed area is characteristic for cubic ice. The bar represents $1 \mu\text{m}$. All the diffractograms are at the same scale given by the position of the 2nd ring of cubic ice [arrow in (d)] corresponding to 4.44 nm^{-1} .

diffractogram undiscernible from the one of vitrified water. This effect takes place with hexagonal as well as with cubic ice and makes that ice crystals are, at low temperature, as delicate as typical organic crystals or biological structures. The only explanation we can propose for this remarkable change is that the apparent high beam resistance of ice observed at higher temperatures, is due to a restoration mechanism which reforms the original structure after the molecule has been displaced or broken by the interaction with the electron. Below 70K the mechanism is blocked at some intermediate stage, thus leaving the damage in the crystal.

The fate of an ice crystal made amorphous by electron irradiation below 70K and rewarmed up to its crystallization temperature is also interesting. After large enough electron irradiation (above 2000 electrons \cdot nm $^{-2}$), the beam-induced "vitrified" ice devitrifies upon rearming as normal H $_2$ O. When, however, irradiation is limited to the dose necessary for "vitrification" but not much more (500 to 2000 electron \cdot nm $^{-2}$), a new phenomenon takes place: when beam-induced "vitrified" hexagonal ice crystals are rewarmed above T $_c$, crystallization does not lead to the usual transformation into small cubic ice crystals, but to the restoration of the original hexagonal crystals. This phenomenon is illustrated in Fig.4 where a thin layer of hexagonal ice crystals spread on a thin carbon film is observed in the scanning transmission electron microscope. Before irradiation, the hexagonal crystals present a rich pattern of bent contours and sharp reflections in the diffractogram. After irradiation at about 40 K, the irradiated region is amorphous but its surroundings remain crystalline. The specimen is then rewarmed to about 155K and the following transformations take place: The central region, irradiated with a dose of 5000 electrons \cdot nm $^{-2}$ takes on the grainy appearance of cubic ice, a structure which is confirmed by the electron diffractogram. The original bent contour reappears in the intermediate region where the specimen was irradiated with 1000 electrons \cdot nm $^{-2}$. The electron diffractograms confirm the reappearance of the original reflections. In this experiment, where the original hexagonal ice crystal is reformed upon rearming of the "vitrified" sample, the memory of the original state is not kept in the non-irradiated part of the original crystal but is inside the apparently amorphous substance. This can be demonstrated when the experiment is made on isolated hexagonal crystals which, after they have been transformed over their whole surface, can still be restored upon warming.

REFERENCES

1. Angell, C.A. (1982) In: Water: A Comprehensive Treatise, F. Franks (ed.), Plenum Press, New York and London, p.1.
2. Brüggeller, P. and Mayer, E. (1980) Nature 288, 569.
3. Dubochet, J. and McDowall, A.W. (1981) J. Microsc. 124, RP3.
4. Adrian, M., Dubochet, J., Lepault, J. and McDowall, A.W. (1984) Nature 308, 32.
5. Dubochet, J., McDowall, A.W., Menge, B., Schmid, E.N. and Lickfeld, K.G. (1983) J. Bacteriol. 155, 381.
6. Dubochet, J., Lepault, J., Freeman, R., Berriman, J.A. and Homo, J.-Cl. (1982) J. Microsc. 128, 219.

7. Dubochet, J., Chang, J.-J., Freeman, R., Lepault, J. and McDowall, A.W. (1982) Ultramicroscopy 10, 55.
8. Dubochet, J., Adrian, M. and Vogel, R.H. (1983) Cryo Letters 4, 233.
9. Lepault, J., Freeman, R. and Dubochet, J. (1983) J. Microsc. 132, RP3.
10. Lepault, J., Booy, F.P. and Dubochet, J. (1983) J. Microsc. 129, 89.
11. Luyet, B. and Rapatz, G. (1958) Biodynamica 8, 1.
12. Dowell, L.G. and Rinfret, A.P. (1960) Nature 188, 1144.
13. Angell, C.A. (1984) Ann. Rev. Phys. Chem. 33, Rabinovitch, B.S. (ed.) Annual reviews Inc., Palo Alto, in press.
14. Ghormley, J.A. and Hochanadel, C.J. (1971) Science 171, 62.
15. Talmon, Y., Davis, H.T., Scriven, L.E. and Thomas, E.L. (1979) J. Microsc. 117, 321.